

IoMT-Based Smart Monitoring Hierarchical Fuzzy Inference System for Diagnosis of COVID-19

Tahir Abbas Khan¹, Sagheer Abbas¹, Allah Ditta², Muhammad Adnan Khan^{3,*},
Hani Alquhayz⁴, Areej Fatima³ and Muhammad Farhan Khan⁵

Abstract: The prediction of human diseases, particularly COVID-19, is an extremely challenging task not only for medical experts but also for the technologists supporting them in diagnosis and treatment. To deal with the prediction and diagnosis of COVID-19, we propose an Internet of Medical Things-based Smart Monitoring Hierarchical Mamdani Fuzzy Inference System (IoMTSM-HMFIS). The proposed system determines the various factors like fever, cough, complete blood count, respiratory rate, Ct-chest, Erythrocyte sedimentation rate and C-reactive protein, family history, and antibody detection (IgG) that are directly involved in COVID-19. The expert system has two input variables in layer 1, and seven input variables in layer 2. In layer 1, the initial identification for COVID-19 is considered, whereas in layer 2, the different factors involved are studied. Finally, advanced lab tests are conducted to identify the actual current status of the disease. The major focus of this study is to build an IoMT-based smart monitoring system that can be used by anyone exposed to COVID-19; the system would evaluate the user's health condition and inform them if they need consultation with a specialist for quarantining. MATLAB-2019a tool is used to conduct the simulation. The COVID-19 IoMTSM-HMFIS system has an overall accuracy of approximately 83%. Finally, to achieve improved performance, the analysis results of the system were shared with experts of the Lahore General Hospital, Lahore, Pakistan.

Keywords: IoMT, MERS-COV, Ct-chest, ESR/CRP, ABD (IgG), Fuzzy logic, HMFIS, WHO.

¹ Department of Computer Science, National College of Business Administration and Economics, Lahore, 54000, Pakistan.

² Department of Information Sciences, Division of Science & Technology, University of Education, Lahore, 54000, Pakistan.

³ Department of Computer Science, Lahore Garrison University, Lahore, 54000, Pakistan.

⁴ Department of Computer Science and Information, College of Science in Zulfi, Majmaah University, Al-Majmaah, 11952, Saudi Arabia.

⁵ Department of Forensic Sciences, University of Health Sciences, Lahore, 54000, Pakistan.

* Corresponding Author: Muhammad Adnan Khan. Email: madnankhan@lgu.edu.pk.

Received: 03 June 2020; Accepted: 23 August 2020.

1 Introduction

The coronavirus disease 2019 (COVID-19) was first reported to the World Health Organization (WHO) country office in China on the 31st of December, 2019. This unknown cause of pneumonia was first registered in Wuhan, China. After analyzing the alarming data and reports received from Wuhan, the WHO declared an international public health emergency on the 30th of January, 2020. As of April 13, 2020, 1,776,867 confirmed cases of COVID-19 have been reported to the WHO; the disease has caused 111,828 deaths globally [Adney, Letko and Ragan (2014)]. Region-wise, the outbreak of this fatal virus has resulted in 913,349 confirmed cases in Europe, 610,741 cases in the USA, 121,710 cases in the Western Pacific, and 102,710 cases in the Eastern Mediterranean. Further, the spread of this pandemic has affected almost all countries worldwide [WHO (2020a, 2020b)].

As these statistics suggest, the outbreak of COVID-19 has proven to be fatal to humans. Medical experts have suggested that COVID-19 may adversely affect the self-immune system resulting in respiratory and severe psychiatric disorders [Li, Guan, Wu et al. (2020)].

Studies from China, Thailand, Japan, and Korea have suggested that the symptoms of COVID-19 appear to be similar to a mild to Severe Acute Respiratory Syndrome (SARS) and as the Middle East Respiratory Syndrome (MERS) [Conzade, Grant, Malik et al. (2018)].

In SARS and MERS cases, age and gender are related to the disease progressing to Acute Respiratory Disorder Syndrome. In the case of MERS, diabetes mellitus, hypertension, malignant growths, renal and lung ailments, and other co-diseases are external factors commonly resulting in a more extreme ailment. Severe Acute Respiratory Coronavirus Syndrome (SARS-CoV) and Middle East Respiratory Coronavirus Syndrome (MERS-CoV) are principally spread from one human to another in medical service settings. Initially, patients report mild symptoms that become increasingly more severe over time. It has been revealed that medical clinics that treated MERS patients were a source of infection to all who visited the clinics [Memish, Cotton, Meyer et al. (2014); Müller, Corman, Jores et al. (2014)].

Studies and field reports on MERS-CoV have demonstrated that infected dromedaries discharge high measures of virus through nasal emissions, although signs of clinical illness are limited to rhinorrhoea and a slight increase in body temperature [Adney, Doremalen, Brown et al. (2014); Khalafalla, Lu, Al-Mubarak et al. (2015)]. Nasal swab tests have indicated that the disease is infectious after the first seven days; in addition, 35 days after contamination, ribonucleic acid (RNA) can still be detected [Doremalen, Hijazeen, Holloway et al. (2017)]. However, examination of camelids and alpacas following vaccination has shown that the virus causing MERS-CoV is extremely host tropic.

The latest technologies in the field of medicine has made it possible to identify the real causes of diseases. This has enabled doctors and other practitioners to identify the risk factors that ultimately lead to a disease, for example, the risk factors of heart disease [Banu (2015)].

Fatima et al. [Fatima, Hussain, Balouch et al. (2020)], presented the IoT-enabled smart monitoring of coronavirus empowered using a fuzzy inference system. However, this

study has few parameters for predicting COVID-19. Further, the accuracy of their proposed model was undetermined.

The current study describes the development of an IoMT-based smart monitoring system that deals with the basic symptoms of COVID-19, suggests risk factors, and provides an efficient evaluation.

A number of studies have been published to investigate diseases in the human body. One such study employed a Fuzzy Inference System (FIS) to investigate and predict the presence of heart disease [Kumar and Kaur (2013)]. The FIS technique for transference of crisp values is generated into fuzzy values. This tool predicts the conditions into two layers of the system having different attributes. Data are thoroughly analyzed from the initial of the disease to final stages.

2 Literature review

The Middle East Reported Coronavirus (MERS-CoV) in 2019 [Adney, Letko, Ragan et al. (2019)]. More than 2300 cases with an expected casualty rate of 35% have been discovered [Adney, Letko, Ragan et al. (2019)]. Dromedary camels have been recognized as the source of zoonotic MERS-CoV transmission in epidemiological investigations, and MERS-CoV appropriation over the first range has been recorded. At present, it remains unknown whether Bactrian camels are defenseless to the disease. Throughout West and Central Asia, the distribution of Bactrian camels is similar to that of dromedary camels. For the 14 build-ups that partner with the MERS-CoV beat receptor, the receptor for MERS-CoV DPP4 of Bactrian camellia appeared in 98.3% of cases, similar to dromedary camel DPP4, which showed a rate of 100% [Adney, Letko, Ragan et al. (2019)].

The causative operator of MERS-CoV in more than 2468 people were analyzed, and more than 851 fatalities have been reported in 27 nations since 2012 [Adney, Letko, Ragan et al. (2019)]. A blend of lopinavir (LPV), ritonavir, and interferonbeta (RTV-IFN β) was considered as a course of treatment for the people in the Kingdom of Saudi Arabia. However, no authorized treatments for MERS-CoV disease have been found. It has been observed, however, that remdesivir and IFN β have a better antiviral activity than LPV and RTV *in vitro*. However, a prophylactic has been shown to be just as helpful in improving the conditions of the lungs in mice and reduce the viral burden and lung ailment in the animals [Adney, Letko, Ragan et al. (2019)]. There is *in vivo* proof of the potential for RDV to treat MERS-CoV contaminations [Sheahan, Sims, Leist et al. (2020)].

Since it was first recognized, the novel COVID-19 plague has spread quickly with cases emerging across China and different nations and locales. Utilizing a transmission model with an estimated essential regenerative number of 3.11 (95% CI=2.39-4.13), 58%-76% of transmissions must be forestalled to stop the expansion. Wuhan reported 83,597 confirmed cases of COVID-19 and 3351 deaths from the disease from April 11 to April 13, 2020 [Read, Bridgen, Cummings et al. (2020)].

In the light of the official declaration of a pneumonia outbreak of obscure etiology having an epidemiological connection to a wet market in Wuhan, China on December 31, 2019, proactive contamination control measures were presented in emergency clinics to contain the spread in Hong Kong. Hong Kong is a cosmopolitan city in southern China with a history of contagious human diseases, such as the avian flu A H5N1 in 1997 and the

serious respiratory disorder related coronavirus (SARS-CoV) in 2003 [Cheng, Wong, To et al. (2020)].

Currently, the modeling, simulation, and optimization of diabetes type II prediction has been conducted using a deep extreme learning machine [Rehman, Athar, Khan et al. (2020)]. The modeling, simulation, and optimization of the diagnosis of cardiovascular disease using computational intelligence methods [Siddiqui, Athar, Khan et al. (2020)] and different assessment questions have been connected with officially existing transformative algorithms [Cheng, Wong, To et al. (2020)], swarm intelligence, a neural network, and fluffy structures [Saleem, Khan, Abbas et al. (2019); Olufunke, Charles, Charles et al. (2013)], which have recently been adopted along with some new methodologies. This has opened different frontiers for researchers regarding the automated diagnosis of Hepatitis-B using a multilayer hierarchical mamdani fuzzy inference system (HMFIS) [Ahmad, Khan, Abbas et al. (2019)].

3 Proposed IoMT-enabled smart monitoring system for COVID-19 disease empowered using HMFIS

In this study, an IoMT-based smart monitoring system for the detection of COVID-19 empowered with HMFIS is proposed. Fig. 1 shows that the proposed model consists of two major modules: (i) a training phase and (ii) a validation phase. Both phases communicate through a cloud.

The training phase consists of three levels: (i) sensory layer, (ii) preprocessing layer, and (iii) application layer. The sensory layer consists of input parameters including fever, cough, CBC, respiratory rate, CT-chest, ESR/CRP, family history, and antibody detection (IgG); the input values are collected and transferred to the database through IoMT. Because wireless communication is applied, the data stored in the database may be inaccurate. The collected data might be noisy and incomplete, and therefore are called raw data. The next layer, called the preprocessing layer, is extremely critical. The deficiencies received through wireless communication in the previous layer can be handled by moving the average and using normalization methods to reduce noisy results. After the preprocessing layer, data are sent to the application layer. The application layer is divided into two sub-layers called the prediction layer and the performance layer. A Hierarchical Fuzzy Inference System (HFIS) is used in the prediction layer to predict the output. The inputs are then collected and transformed into a fuzzy set with fuzzy linguistic variables and fuzzy membership functions. Fuzzy modifications will be made by the HFIS. The prediction layer sends the predicted information to the next phase called the performance layer. In the performance layer, the performance regarding the data received from the prediction layer is evaluated.

The results of the performance layer are compared based on the accuracy and error rate achieved by the HFIS. After a comparison of the results, “Yes” indicates that COVID-19 was successfully detected, and “No” indicates that the prediction layer will be updated until the learning criteria are met. The results are then moved to a database residing in a cloud for further importation to the FIS for prediction.

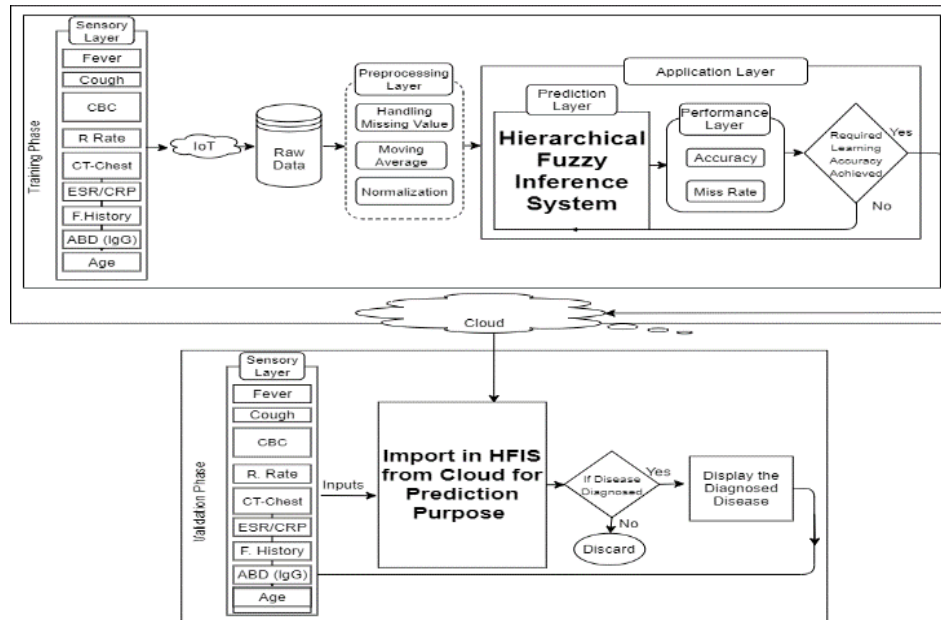


Figure 1: Proposed IoMT-enabled smart monitoring system for COVID-19 disease empowered using HMFIS

The accuracy and error rate are taken into account. This process is continued until the required accuracy is achieved. After achieving the required accuracy, the HMFIS is uploaded to the cloud. The last phase is the validation phase. In this phase, the trained HMFIS is imported for prediction to validate whether the patient is infected with COVID-19 based on the results.

In Fig. 2, a flow diagram of how COVID-19 detection is to be performed has been issued by the government of Punjab is shown. This flowchart has been designed by a specialized healthcare and medical education center in Lahore, Pakistan, is shown. In Fig. 2, different parameters are identified for COVID-19 patients; the treatment flow chart for different stages of the disease is also shown. Most of the parameters in IoMTSM-HMFIS are taken from this official algorithm.

3.1 Hierarchical mamdani fuzzy inference system

As shown in Fig. 3, HFIS is able to predict COVID-19 cases. HMFIS is mounted in the prediction layer. If the sensory layer input parameters are applicable, they will move to the next phase by converting inputs through fuzzification into fuzzy crisp inputs. A crisp set of input data is attained and converted into a fuzzy set by the help of fuzzy linguistic variables, semantic terms, and membership functions. This process continues through the HFIS during the next phase.

3.1.1 Input variables

First, the proposed system collects data regarding COVID-19 disease. Later, we transform these real data into fuzzy input variables, which is our core method used to

evaluate the real risk factors. These fuzzy variables are the statistical values used in our algorithm to identify the risk factors and their effects on the human body. In this study, nine fuzzy variables are used. The details of these fuzzy variables are shown in Tab. 1.

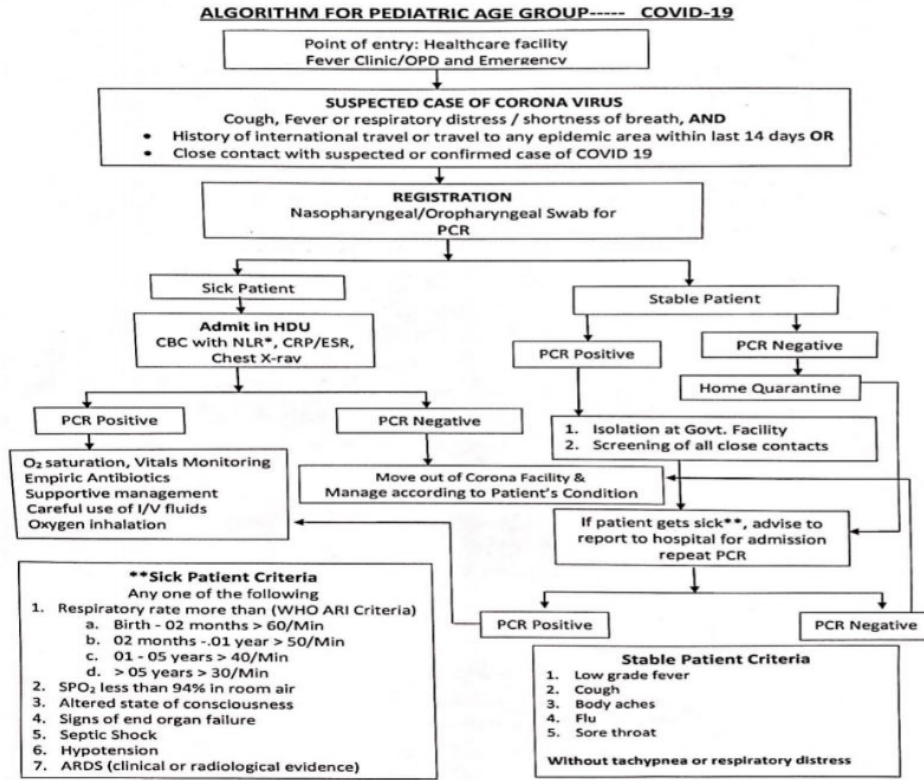


Figure 2: Flow diagram of COVID-19 detection issued by the Government of Punjab at a specialized healthcare and medical education center, Lahore, Pakistan

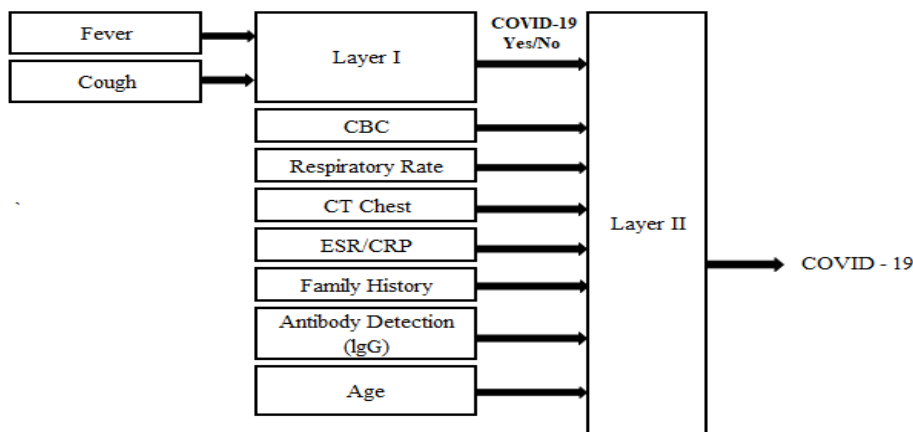


Figure 3: Hierarchical mamdani fuzzy inference system

Table 1: Input variables

Sr. #	Input field	Limits	Semantic representation
1	Fever	1	Low-grade temp (99°C to 102°C)
		2	Moderate-grade temp (101.5°C to 104°C)
		3	High-grade temp (103.5°C to 106°C)
2	Cough	1	Good
		2	Normal
		3	Abnormal
3	CBC	1	Normal (35,00-10,500) cell/mcl
		2	Abnormal (above)
4	Respiratory Rate	1	Normal (14-17)
		2	Moderate (18-20)
		3	Abnormal (<20)
5	CT Chest/ RT-PCR	1	Positive
		2	Negative
6	ESR/CRP	1	Normal (≥ 50)
		2	Moderate (51-100)
		3	Abnormal (<100)
7	Family History	1	Yes
		2	No
8	Antibody Detection (IgG)	1	Normal (0.8-2.0)
		2	Moderate (2.1-4.4)
		3	Abnormal (4.5-12.9)
9	Age	18-35	Young
		36-50	Middle-aged
		50>	Elderly

3.1.2 Output variables

The output variables are directly dependent on the fuzzy input variables and are used to show the response of the latter. The detailed responses of the fuzzy input variables are shown in Tab. 2.

Table 2: Output variables

Sr#	Range	Output representation
1	>0.5	(No COVID-19)
	0.5= >	(Yes COVID-19)

3.1.3 Member function

In Tab. 3, the membership function is used to produce a curve value between 0 and 1 and as well as a mathematical function for analyzing the statistical values of the fuzzy input

and output variables. The proposed FIS model, called IoMT-enabled smart monitoring of COVID-19, is graphically and mathematically presented in Tab. 1. The rows (2-7) present the input member functions and row (8) presents the output member function.

3.1.4 Knowledge-based rule

The fuzzy inference system is mainly adopted and applied to fuzzy input sets and fuzzy logic as a tool for extracting the results in Tab. 1 for the inputs and those in Tab. 3 for the member function representation of their behavior. This knowledge-based system is shown in Fig. 3.

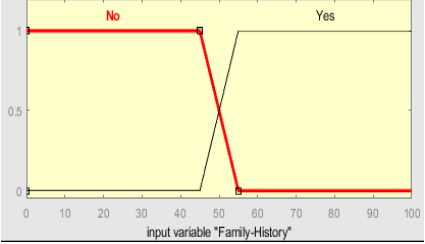
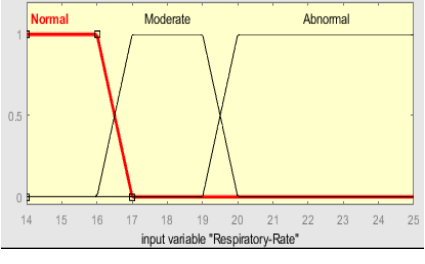
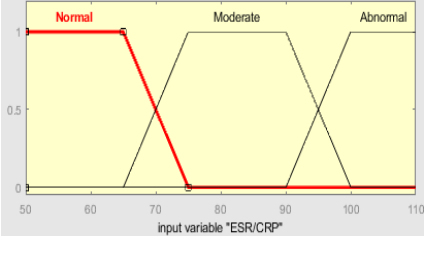
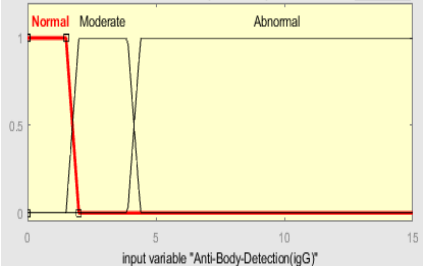
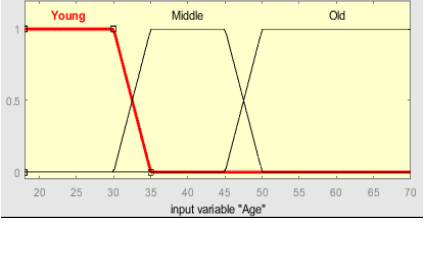
3.1.5 De-fuzzier

After applying the fuzzy crisp rules on the given inputs, a FIS generates the outputs by accepting the fuzzy sets along with the degrees of the member function. Different types of de-fuzzifiers are applied to achieve better results. In this study, a centroid de-fuzzifier is applied. A graphical representation of the FIS is shown in Fig. 3.

In Fig. 4, a 3D view of the ruled surface of the proposed model is applied to the CBC and CT-chest/RT-PCR. In Fig. 5, the 3D view of the ruled surface of the proposed model is applied to the CBC and family history. In Fig. 6, the 3D view of the ruled surface of the proposed model is applied to the ESR/CRP and respiratory rate. In Fig. 7, the 3D view of the ruled surface of the proposed model is applied to ESR/CRP and age. Finally, in Fig. 8, the 3D view of the ruled surface of the proposed model is applied to age and CT-chest/RT-PCR. For all figures, the simulation results in yellow are considered good, the results in green are satisfactory, and the results in blue are poor.

Table 3: Input/output variables, member functions, and graphical representation

Input/output	Membership Function	Graphical Representation of MF
CBC $= \mu_{CBC}(cbc)$	$\mu_{CBC,No}(cbc)$ $= \{\max(\min(1, \frac{35 - cbc}{15}), 0)\}$ $\mu_{CBC,Yes}(cbc)$ $= \{\max(\min(\frac{50 - cbc}{15}, 1), 0)\}$	
CTC $= \mu_{CTC}(ctc)$	$\mu_{CTC,No}(ctc)$ $= \{\max(\min(1, \frac{45 - ctc}{15}), 0)\}$ $\mu_{CTC,Yes}(ctc)$ $= \{\max(\min(\frac{60 - ctc}{15}, 1), 0)\}$	

FH $= \mu_{FH}(fh)$	$\mu_{FH,No}(fh) = \{\max(\min(1, \frac{45 - fh}{10}), 0)\}$ $\mu_{FH,Yes}(fh) = \{\max(\min(\frac{55 - fh}{10}, 1), 0)\}$	
$RR = \mu_{RR}(rr)$	$\mu_{RR, Normal}(rr) = \{\max(\min(1, \frac{16 - rr}{1}), 0)\}$ $\mu_{RR, Moderate}(rr) = \{\max(\min(\frac{rr - 16}{1}, 1, \frac{20 - rr}{1}), 0)\}$ $\mu_{RR, Abnormal}(rr) = \{\max(\min(\frac{20 - rr}{1}, 1), 0)\}$	
ESR $= \mu_{ESR}(esr)$	$\mu_{ESR, Normal}(esr) = \{\max(\min(1, \frac{65 - esr}{10}), 0)\}$ $\mu_{ESR, Moderate}(esr) = \{\max(\min(\frac{esr - 65}{10}, 1, \frac{100 - esr}{10}), 0)\}$ $\mu_{ESR, Abnormal}(esr) = \{\max(\min(\frac{100 - esr}{10}, 1), 0)\}$	
ABD $= \mu_{ABD}(abd)$	$\mu_{ABD, Normal}(abd) = \{\max(\min(1, \frac{1 - abd}{0.5}), 0)\}$ $\mu_{ABD, Moderate}(abd) = \{\max(\min(\frac{abd - 1}{0.5}, 1, \frac{4.4 - abd}{0.5}), 0)\}$ $\mu_{ABD, Abnormal}(abd) = \{\max(\min(\frac{4.4 - abd}{0.5}, 1), 0)\}$	
$A = \mu_A(a)$	$\mu_{A, Young}(a) = \{\max(\min(1, \frac{30 - a}{5}), 0)\}$ $\mu_{A, Middle}(a) = \{\max(\min(\frac{a - 30}{5}, 1, \frac{50 - a}{5}), 0)\}$ $\mu_{A, Old}(a) = \{\max(\min(\frac{50 - a}{5}, 1), 0)\}$	

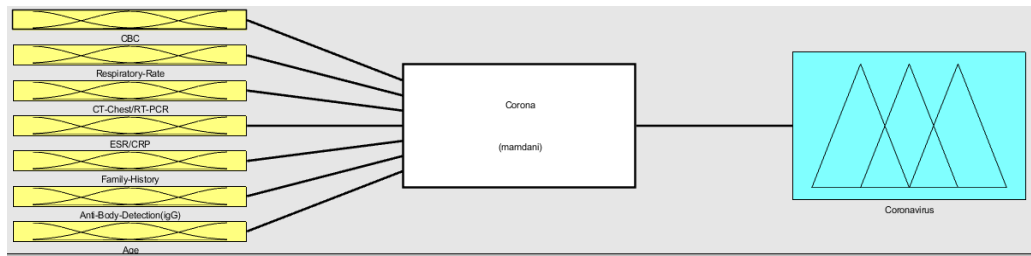
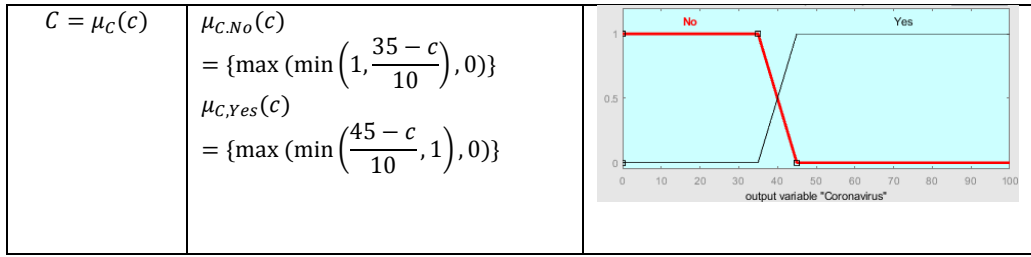


Figure 3: Proposed HMFIS for COVID-19

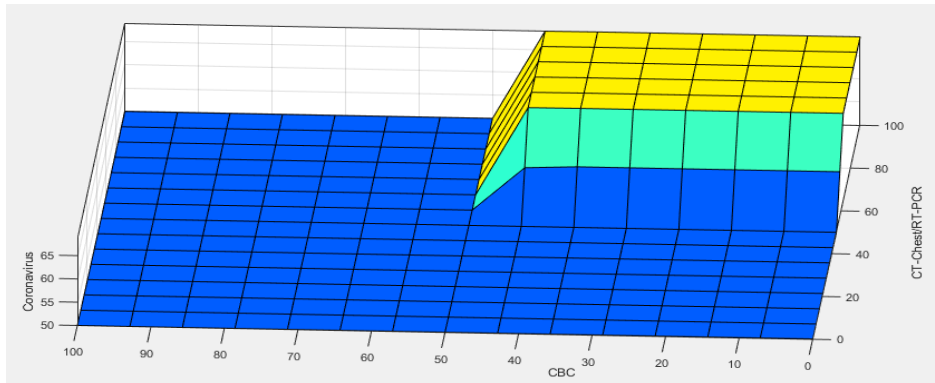


Figure 4: Rule surface of proposed IoMTSM-HMFIS on CBC and CT-chest

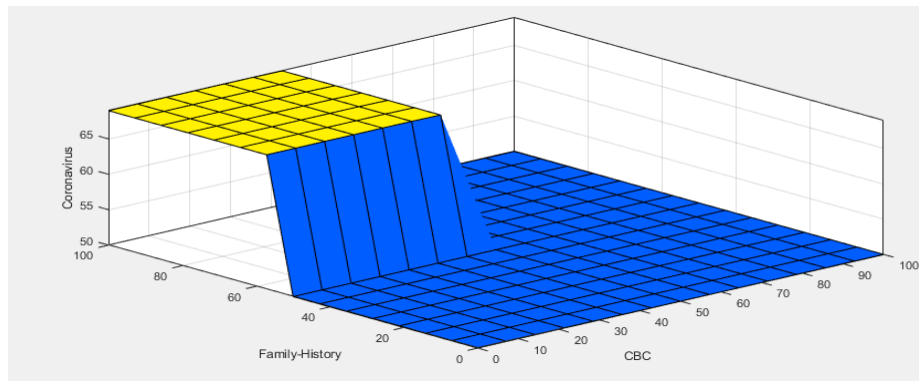


Figure 5: Rule surface of proposed IoMTSM-HMFIS on CBC and family history

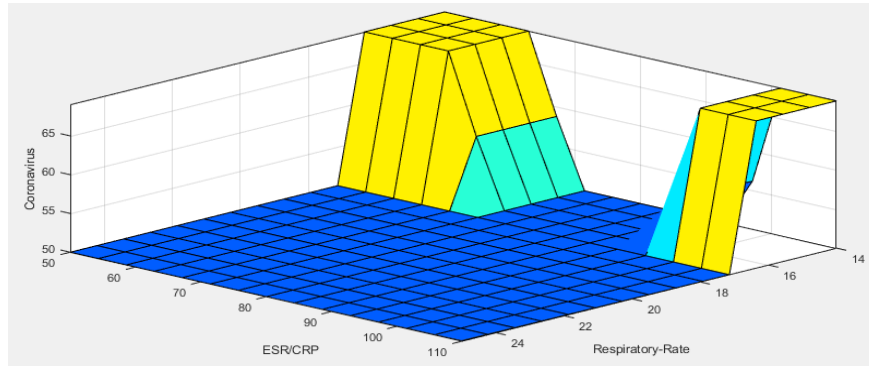


Figure 6: Rule surface of proposed IoMTSM-HMFIS on ESR/CRP and RR

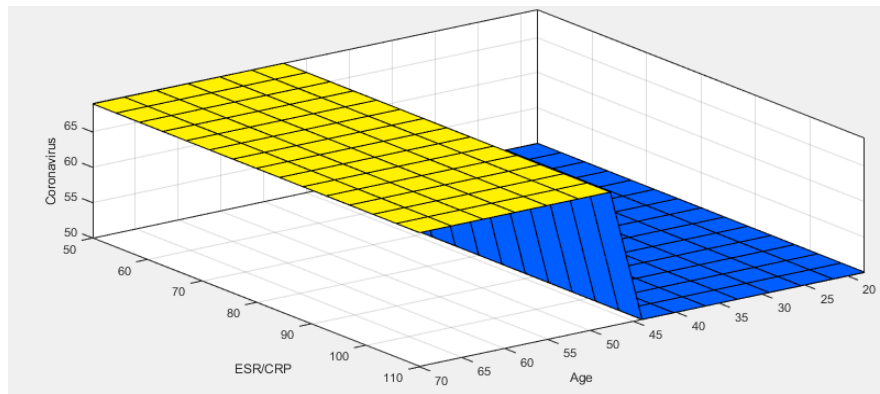


Figure 7: Rule surface of proposed IoMTSM-HMFIS on ESR/CRP and age

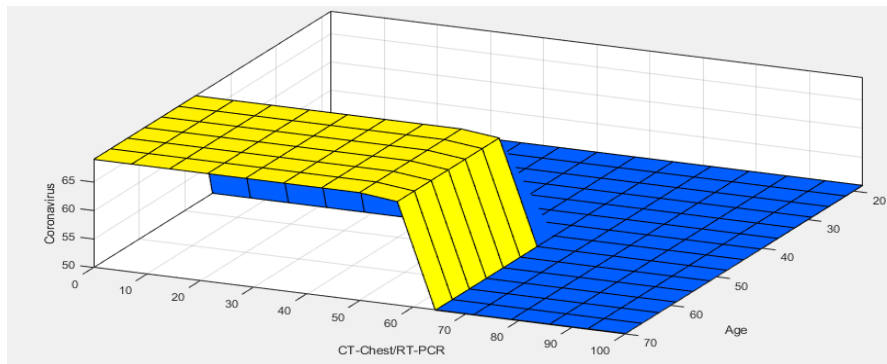


Figure 8: Rule surface of proposed IoMTSM-HMFIS on age and CT-chest/RT-PCR

Simulation results of proposed IoMT-based smart monitoring system are empowered using HMFIS. The MATLAB R2019a tool is utilized for the simulation results. MATLAB is similarly utilized for modeling, prototyping, simulation, algorithm extension, and many other aspects. For the reproduction results, seven data sources and one output factor are utilized. In this study, the proposed FIS demonstrates the different types of

output, such as the IoMT-based SMFIS system for prediction. The lookup rules diagram is generated using the FIS designer.

Fig. 9 shows that if the input value of CBC is “Normal,” RR is “Normal,” CT-chest/RT-PCR is “Negative,” ESR/CRP is “Normal,” family history is “No,” ABD (IgG) is “Normal,” and age is “Young,” then the COVID-19 prediction is “No.” Fig. 10 shows that if the input value of CBC is “Normal,” RR is “Abnormal,” CT-chest/RT-PCR is “Positive,” ESR/CRP is “Abnormal,” Family History is “No,” ABD (IgG) is “Abnormal,” and age is “Elderly,” then the COVID-19 prediction is “Yes.” Tab. 4 shows the accuracy of the proposed IoMTSM-HMFIS expert system in comparison with the medical human expert of the general hospital in Lahore, Pakistan. The accuracy of the proposed method is randomly checked on 40 records. During the simulation, we considered different numeric ranges based on “Normal,” “Moderate,” and “Abnormal” in most cases, and in some cases, we considered their presence using “Yes/No” and “Positive/Negative.”

The proposed expert IoMTSM-HMFIS system provides accurate results for all cases and shows minor errors only at the borderline owing to the possibilities of both outcomes.



Figure 9: Lookup diagram of proposed IoMTSM-HMFIS (No)



Figure 10: Lookup diagram of proposed IoMTSM-HMFIS (Yes)

Fig. 11 shows the precision of the proposed expert IoMTSM-HMFIS system in terms of the probability of all output cases. The first column represents the accuracy of non-COVID-19 patients, which is 91%, and the second column represents the accuracy of patients with COVID-19, which is 71%. The last column represents an overall accuracy of the proposed IoMTSM-HMFIS expert system, which is 82.5%.

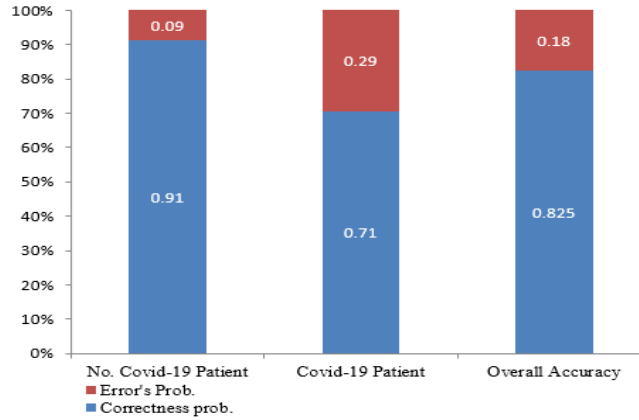


Figure 11: Precision of proposed expert IoMTSM-HMFIS system

Table 4: Accuracy of the proposed expert IoMTMS-HMFIS system

P	CBC	RR	CT-Chest	ESR/CRP	Family History	ABD	Age	HED	PMD	PC	PE
1	N (5.5)	N (15.2)	N (17.5)	N (64.7)	N (15.5)	N (3.75)	Y (25.5)				
2	N (9.7)	N (18)	N (22)	N (64.7)	N (15.5)	M (2.48)	Y (25.5)				
3	N (18)	N (12)	N (22)	N (64.7)	N (25.5)	M (3.08)	Y (25.5)				
4	N (5.5)	N (15.2)	N (17.5)	N (64.7)	N (15.5)	N (3.75)	Y (25.5)				
5	N (5.5)	N (15.2)	N (44.5)	N (64.7)	N (15.5)	M (2.48)	Y (25.5)				
6	N (5.5)	N (15.2)	N (44.5)	N (64.7)	N (25.5)	M (3.08)	Y (25.5)				
7	N (5.5)	N (15.2)	N (44.5)	N (64.7)	N (25.5)	A (7.84)	Y (25.5)				
8	N (5.5)	N (15.2)	N (16.5)	M (89.9)	N (24.5)	N (1.43)	Y (25.5)				
9	N (5.5)	N (15.2)	N (16.5)	M (89.9)	N (24.5)	N (1.43)	M (38.5)				
10	N (5.5)	N (15.2)	N (16.5)	N (59.3)	N (24.5)	N (1.43)	M (38.5)				
11	N (11)	N (15.2)	N (16.5)	N (59.3)	N (5.5)	A (9.52)	M (41.7)		No		9.0
12	N (11)	N (14.9)	N (16.5)	N (58.7)	N (35.5)	A (9.52)	M (41.7)	No		91.0	
13	N (11)	N (14.9)	N (16.5)	N (58.7)	N (35.5)	A (9.52)	Y (25.5)				
14	N (11)	N (14.9)	N (13.5)	N (53.9)	N (35.5)	A (9.52)	Y (25.5)				
15	N (24)	N (15.4)	N (13.5)	M (84.9)	N (35.5)	A (9.52)	Y (25.5)				
16	N (24)	N (15.4)	N (13.5)	M (84.9)	N (35.5)	M (3.38)	Y (24.5)				
17	N (24)	N (15.4)	N (13.5)	N (61.7)	N (35.5)	M (3.38)	Y (24.5)				
18	N (12)	N (15.4)	N (13.5)	N (61.7)	N (12.5)	M (3.38)	Y (24.5)				
19	N (23)	N (15.4)	N (13.5)	N (61.7)	N (34.5)	N (9.75)	Y (28.7)				
20	N (23)	N (15.4)	N (13.5)	N (53.9)	N (15.5)	M (2.63)	Y (28.7)				
21	N (23)	N (15.4)	N (13.5)	N (61.1)	N (34.5)	M (2.63)	Y (26.1)				
22	N (41)	N (15.4)	N (37.5)	N (61.1)	N (34.5)	M (2.63)	Y (26.1)		Yes		
23	N (41)	N (15.4)	N (18.5)	M (80.3)	N (34.5)	M (2.63)	Y (26.1)		Yes		
24	A (70)	N (16.1)	P (76.5)	A (103)	N (50)	A (7.50)	M (44)				
25	N (36)	N (15.9)	N (37.5)	N (65.3)	Y (86.5)	M (2.77)	Y (26.6)				
26	A (70)	N (16.1)	P (76.5)	A (103)	Y (83.5)	M (3.38)	O (57.8)				
27	N (13)	N (15.6)	N (28.5)	M (82.7)	Y (83.5)	N (.825)	O (58.6)				
28	N (13)	N (15.6)	N (16.5)	M (82.7)	Y (83.5)	N (1.42)	O (64)				
29	N (13)	N (15.6)	N (51.5)	M (82.7)	Y (83.5)	N (1.42)	O (64)				
30	N (13)	N (15.6)	N (40.5)	M (82.7)	Y (83.5)	M (3.67)	O (64)				
31	N (13)	N (15.6)	N (40.5)	M (82.7)	Y (54.5)	M (3.67)	O (64)	Yes	Yes	71.0	29.0
32	N (35)	N (15.6)	N (20.5)	M (82.7)	Y (54.5)	M (3.67)	O (64)				
33	N (35)	N (15.6)	N (20.5)	M (88.7)	Y (54.5)	A (10.7)	M (39.1)		No		
34	N (35)	N (15.6)	N (30.5)	M (88.7)	Y (81.5)	A (14.8)	M (39.1)		No		
35	N (35)	N (15.6)	N (9.5)	M (88.7)	Y (81.5)	A (14.8)	M (39.1)		Yes		
36	N (35)	N (14.1)	N (31.5)	M (88.7)	Y (86.5)	M (2.77)	Y (30.1)		No		
37	N (35)	N (14.1)	N (37.5)	M (85.7)	Y (86.5)	N (1.13)	Y (26.6)		Yes		
38	N (35)	N (16.1)	N (37.5)	M (85.7)	Y (86.5)	N (.525)	Y (26.6)		No		
39	N (20)	N (14.7)	N (37.5)	M (56.3)	Y (86.5)	N (.525)	Y (26.6)		No		
40	N (37)	N (15.9)	N (37.5)	M (65.3)	Y (86.5)	N (.525)	Y (26.6)		Yes		

P=Patient, RR=Respiratory Rate, ABD=Antibody Detection (IgG), HED=Human Expert Decision, PMD=Proposed Model Decision, PC=Probability of Correctness, PE=Probability of Error

4 Conclusion and future studies

A proposed IoMT-based smart monitoring system empowered with HMLFIS was introduced to monitor COVID-19 in a quick and efficient manner. The proposed IoMT-based smart monitoring HMFIS system effectively monitors the affected patients and identifies whether the patient is a victim of COVID-19. The detection of patients unaffected by COVID-19 is 91.3%. The patients affected by COVID-19, but detected by the system as non-COVID-19 patients is 70.5%, which is not good and is because of the novelty of the disease. However, the overall precision of our proposed system is 82.5% and it can be improved in the future by applying deep extreme learning algorithms and neuro-fuzzy systems. The proposed IoMT-based FIS system uses MATLAB 2019a for the simulations. The simulation results of the proposed system were shown to be accurate.

Funding Statement: The author(s) received no specific funding for this study.

Conflicts of Interest: The authors declare that they have no conflicts of interest to report regarding the present study.

References

- Adney, D. R.; Letko, M.; Ragan, I. K.; Scott, D.; van Doremalen, N. et al.** (2019): Bactrian camels shed large quantities of middle east respiratory syndrome coronavirus after experimental infection. *Emerging Microbes and Infections*, vol. 8, no. 1, pp. 717-723.
- Adney, D. R.; van Doremalen, N.; Brown, V. R.; Bushmaker, T.; Scott, D. et al.** (2014): Replication and shedding of MERS-CoV in the upper respiratory tract of inoculated dromedary camels. *Emerging Infectious Diseases*, vol. 20, no. 12, pp. 1999-2005.
- Ahmad, G.; Khan, M. A.; Abbas, S.; Athar, A.; Khan, B. S. et al.** (2019): Automated diagnosis of hepatitis b using multilayer Mamdani fuzzy inference system. *Journal of Healthcare Engineering*, vol. 2019, pp. 1-15.
- Banu, G. R.** (2015): Predicting heart attack using fuzzy c means clustering algorithm. *IOSR Journal of Computer Engineering*, vol. 5, no. 3, pp. 439-443.
- Cheng, V. C.; Wong, S. C.; To, K. K.; Ho, P. L.; Yuen, K. Y. et al.** (2020): Preparedness and proactive infection control measures against the emerging Wuhan coronavirus pneumonia in China. *Journal of Hospital Infection*, vol. 104, no. 3, pp. 254-255.
- Conzade, R.; Grant, R.; Malik, M. R.; Elkholy, A.; Elhakim, M. et al.** (2018): Reported direct and indirect contact with dromedary camels among laboratory-confirmed MERS-CoV cases. *Viruses*, vol. 10, no. 8, pp. 425-433.
- Fatima, S. A.; Hussain, N.; Balouch, A.; Rustam, I.; Saleem, M. et al.** (2020): IoT enabled smart monitoring of coronavirus empowered with fuzzy inference system. *International Journal of Advanced Research, Ideas, and Innovations in Technology*, vol. 6, no. 1, pp. 1-10.
- Khalafalla, A. I.; Lu, X.; Al-Mubarak, A. I. A.; Dalab, A. H. S.; Al-Busadah, K. A. S. et al.** (2015): MERS-CoV in the upper respiratory tract and lungs of dromedary camels, Saudi Arabia, 2013-2014. *Emerging Infectious Diseases*, vol. 21, no. 7, pp. 1153-1157.

Kumar, S.; Kaur, G. (2013): Detection of heart diseases using fuzzy logic. *International Journal of Engineering Trends and Technology*, vol. 4, no. 6, pp. 2694-2699.

Li, Q.; Guan, X.; Wu, P.; Wang, X.; Zhou L. et al. (2020): Early transmission dynamics in Wuhan, China, of novel coronavirus-infected pneumonia. *New England Journal of Medicine*.

Memish, Z. A.; Cotton, M.; Meyer, B.; Watson, S. J. et al. (2014): Human infection with MERS coronavirus after exposure to infected camels, Saudi Arabia, 2013. *Emerging Infectious Diseases*, vol. 20, no. 6, pp. 1012-1018.

Müller, M. A.; Corman, V. M.; Jores, J.; Meyer, B.; Younan, M. et al. (2014): MERS coronavirus neutralizing antibodies in camels, Eastern Africa, 1983-1997. *Emerging Infectious Diseases*, vol. 20, no. 12, pp. 2093-2099.

Olufunke, O. O.; Charles, U. O.; Charles, A. K.; Abraham, A. et al. (2013): A fuzzy-mining approach for solving rule-based expert system unwieldiness in the medical domain. *Neural Network World*, vol. 23, no. 5, pp. 435-450.

Read, J. M.; Bridgen, J. R.; Cummings, D. A.; Ho, A.; Jewell, C. P. et al. (2020): Novel coronavirus 2019-nCoV: early estimation of epidemiological parameters and epidemic predictions. *MedRxiv*.

Rehman, A.; Athar, A.; Khan, M. A.; Abbas, S.; Fatima, A. et al. (2020): Modelling, simulation, and optimization of diabetes type II prediction using deep extreme learning machine. *Journal of Ambient Intelligence and Smart Environments*, vol. 12, no. 2, pp. 125-138.

Saleem, M.; Khan, M. A.; Abbas, S.; Asif, M.; Hassan, M. et al. (2019): Intelligent fso link for communication in natural disasters empowered with fuzzy inference system. *In 2019 International Conference on Electrical, Communication, and Computer Engineering*, IEEE, pp. 1-6.

Sheahan, T. P.; Sims, A. C.; Leist, S. R.; Schäfer, A.; Won, J. et al. (2020): Comparative therapeutic efficacy of remdesivir and combination lopinavir, ritonavir, and interferon-beta against MERS-CoV. *Nature Communications*, vol. 11, no. 1, pp. 114-117

Siddiqui, S. Y.; Athar, A.; Khan, M. A.; Abbas, S.; Saeem, Y. et al. (2020): Modelling, simulation, and optimization of diagnosis of cardiovascular disease using computational intelligence approaches. *Journal of Medical Imaging and Health Informatics*, vol. 10, no. 5, pp. 1005-1022.

Van Doremalen, N.; Hijazeen, Z. S.; Holloway, P.; Al Omari, B.; McDowell, C. et al. (2017): High prevalence of middle east respiratory coronavirus in young dromedary camels in Jordan. *Vector-Borne and Zoonotic Diseases*, vol. 17, no. 2, pp. 155-159.

<https://www.who.int/emergencies/diseases/novel-coronavirus-2019/events-as-they-happen>

<https://who.sprinklr.com/region/wpro/country/cn>